

Study on nuclear and renewable hybrid energy system performance prediction by using Modelica

Sungho Kim^a, Daehoh Kang^b, Kyungrim Ahn^b, Juhyeong Park^b, Hae-Ryong Hwang^{c*}

^aKEPCO E&C, 1113, Daedeok-daero 989beon-gil, Yuseong-gu, Daejeon, Republic of Korea, 34057

^biVH, 19, Yangjaecheon-ro 17-gil, Seocho-gu, Seoul, Republic of Korea, 06754

^cISMR, 210, Dongho-ro, Jung-gu, Seoul, Republic of Korea, 04601

*Corresponding author: harold.hwang@ismr.co.kr

1. Introduction

The production and use of electric energy is constantly evolving in the building, industrial and transportation areas [1,2].

Looking at the electric energy production sector, the market share of variable renewable energy such as wind and solar power (PV) is continuously increasing.

Among the use sectors, the transportation area is encouraged to use eco-friendly fuels, and accordingly, the use rate of battery and hydrogen electric fuel vehicles is rapidly increasing. In the building area, energy efficiency is increasing due to building energy management system (BEMS) and high-insulation materials.

Since 2010, researches in nuclear-renewable hybrid energy system (NRHES) have been actively conducted to maximize efficiency in electric energy production and use.

The NR HES, which combines production and use, is a system that actively controls electricity production and use and surplus energy utilization [3].

In this study performance analysis is performed for the architecture depicted in the former study[3] by digital twin for securing operation efficiency of NRHES.

Digital twin is built based on multi-physics system using Modelica. All components were modeled to consider electricity, heat, mechanics and environment at the same time[4,5].

2. Methods and Results

This study was proceeded in two stages for the evaluation of the efficiencies of three proposed architectures of NRHES. The first step is to build an NRHES digital twin using Modelica. Renewable energy consists of solar and wind power. Nuclear power consists of a steam generator and a turbine generator. Energy is stored in battery energy storage system(ESS) and Thermal storage. The industrial process produces hydrogen. Only low temperature water electrolysis (LTE) was considered in this study.

The second step is to define scenarios for each energy storage method and predict the optimal architecture through efficiency analysis. There are three scenarios used. The first is to use only battery ESS, and the second is to use the battery ESS and the low-temperature water electrolysis (LTE) at the same time. Finally, battery ESS, LTE, and thermal storage are added all together.

2.1. Digital twin construction of NRHES system

As shown in Figure 2.1 and Table 2.1, NRHES is composed of renewable energy block, nuclear energy block, energy storage block, industrial process block, demand load block and controller. The detailed modeling method for each block is as in the subsection. All module m

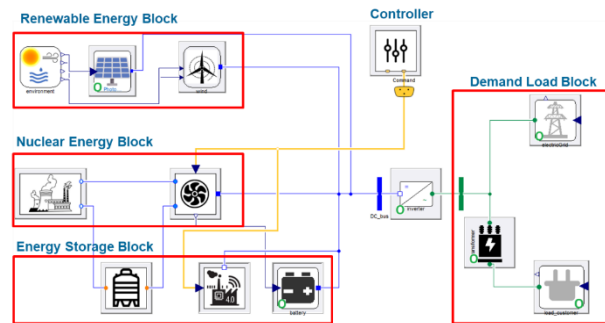


Fig 2.1. NRHES architecture

Table 2.1 NRHES sub-module list

Part Name	Content
Nuclear steam generator	Steam production model with heat from reactor
PV panel	Solar Photon-powered models
Wind turbine	Power generation model with wind velocity as input
ESS	ESS Model using battery
IP (electrolyzer)	Hydrogen model in LTE method
Thermal storage	Heat storage model with salt water as medium

2.1.1. Nuclear Steam Generator

The steam generator is a key component for the operation and the safety of the plant because it is responsible for the generating steam and cooling of the reactor.

Water and steam flow is as follows. The primary water flows into U-tubes and yields its heat to the secondary water. The secondary water, circulating outside the U-tubes, is liquid at the inlet of the steam generator, then flows down the outer part of the steam generator and

starts to boil when reaching the bottom center part of the steam generator, until the top of the boiling section. There, the ratio between the total flow rate and steam flow rate (circulation rate) reaches a value of 4 to 5 at nominal power.

This part of the steam generator is called the riser, where the flow is mainly two-phase (a mixture of water and steam). Moreover, due to the non-homogeneity of heat exchange inside the riser, two regions must be considered. When secondary water is flowing outside the first half part of U-tubes with hot primary water flowing in, the region is called “hot leg”. When flowing outside the other half part of U-tubes with cooler primary water flowing in, the regions is called “cold leg”.

The water and steam mixture passes then through separators where the two phases are separated in the upper part of the steam generator. The liquid part goes back to the steam generator feedwater, and the vapor part goes to the turbine. This part of the steam generator is called the dome.

The thermal load on the riser tube increases at $t=500$. This increases the pressure initially before the pressure controller increases the opening of the high-pressure steam valve to control the pressure back to the set point, increasing the steam flow and increasing the production power.

The current model produces $275\text{ }^{\circ}\text{C}$ of steam from nuclear energy block. The main steam is produced by the reactor and controlled by the auxiliary heat source, using default parameters for pumps and capacitors.

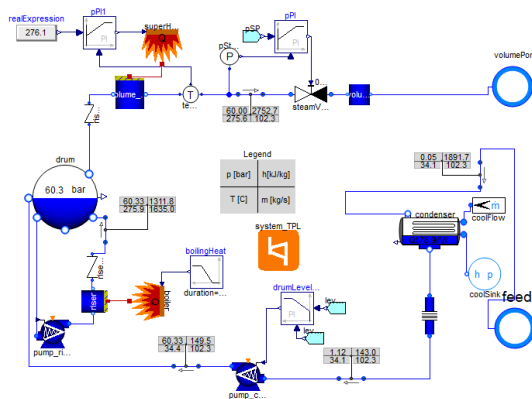


Fig 2.2 Close loop steam cycle

As a result of model verification, the nuclear steam generator produces 60.8 MW of electric power, which predicts approximate results with the specifications of 60.0 MW. A comparison of the physical quantities at key points is shown in Table 2.2.

Table 2.2 Comparison of steam cycle state with reference data

Location	Variable	Model	Reference	Error
Turbine inlet	Temperature	275.6	276.0	0%
	Pressure	60.0	60.0	0%
	Enthalpy	2752.0	2787.0	1%
	Mass flow rate	102.3	102.7	0%
Turbine outlet	Temperature	34.1	43.0	21%
	Pressure	0.057	0.086	34%
	Enthalpy	1892.0	1838.0	-3%
	Mass flow rate	102.3	74.5	-37%

2.1.2. Wind turbine

The wind turbine components take wind speed data as input and carry the power generated based on the given parameters.

The main model parameters are summarized as follows:

- 1) Environmental factors: Typical values of air density, reference height and friction coefficients for which wind speed is measured, and friction coefficients for different areas are shown in Figure 2.3.
- 2) Shape of wind turbine: hub height and blade length L (Own area A is calculated based on blade length). Rated power capacity, the rated wind speed is calculated from the given correlation.
- 3) Cut-in and cut-out wind speeds: represent the operating conditions of the turbine.
- 4) The total power is calculated to reflect efficiency.

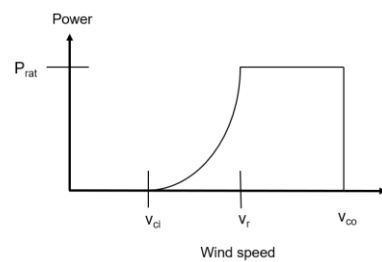


Fig 2.3. Turbine model

Between the cut-in and rated speeds, the power is calculated as follows.

$$P_{calc} = P_{rat} \cdot \frac{(v^3 - v_{ci}^3)}{v_{rat}^3 - v_{ci}^3} \quad (1)$$

$$P_{wind} = P_{calc} \cdot \eta \quad (2)$$

As a result of the model verification, the power output per hour of the prediction and reference was found very similar.

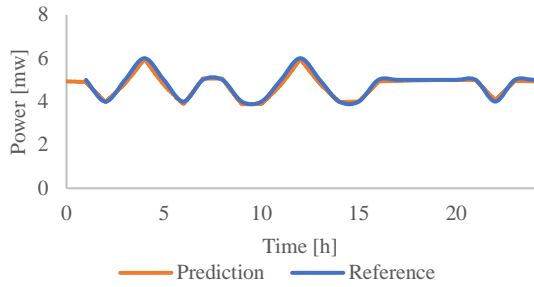


Fig 2.4. wind power correlation results

2.1.3. Photovoltaics Power

The solar module and array generate DC power and are next connected to DC-AC inverter. Inverters typically contain control logic to regulate the DC voltage of the photovoltaic module. This is typically a Maximum Power Point Tracker (MPPT).

Solar modules do not generate the same amount of power for a given environmental boundary condition (mostly illuminance, temperature, and air mass). In fact, the power depends on the DC voltage of the module pin. This is easily understood by considering the 0V voltage drop between the pins. Whatever the current is, the power becomes zero. However, in grid applications, power sources such as solar modules must provide optimal power. Therefore, the DC voltage should be set to a value that maximizes the power of the module.

This model allows you to extract the maximum power point analytically from the equation. This prevents the inverter DC voltage from being set using an external controller (tracer), which is typically computationally expensive.

When MPPT is enabled, the current on the pin corresponding to the module operating at the maximum power point is set.

When MPPT (default) is disabled, the actual current corresponding to the voltage set on the pin is provided. This still allows you to analytically extract the maximum power point voltage and output it via real output, but a feedback loop (mostly via an inverter) is required to set the voltage at this value.

Power output depends on solar radiation and the efficiency of the solar components. The mitigation factor eta is defined as a parameter that depends on PV component aging, wiring loss, and dust cover.

$$P(t) = P_{rat} \cdot \eta_{PV} \cdot G(t)[1 + \alpha_{PV} \cdot (T_{PV} - 298.15)] \quad (3)$$

$$T_{PV} = \frac{T_{ambient} + A \cdot \Gamma}{1 + B \cdot \Gamma}$$

$$A = 1 - \frac{\eta_{STC}(1 - 25\alpha_{TP})}{0.9}$$

$$B = \frac{\alpha_{TP} \cdot \eta_{STC}}{0.9}$$

$$\Gamma = \frac{(T_{NOCT} - 293.15)G(t)}{0.8}$$

Based on the results of the reference, the model verification confirmed that the power output per hour was more than 98% consistent.

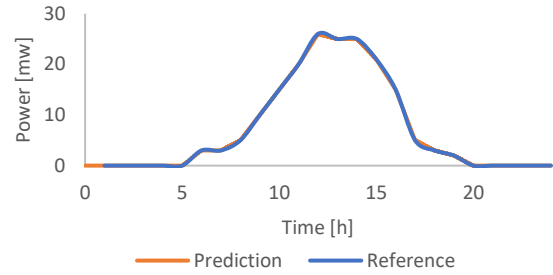


Fig 2.5. PV panel correlation results

2.1.4 Industrial Process(IP)

This is an alkaline electrolyte model for use in the microgrid optimization framework. This model has the following connectors:

- Fluid ports for hydrogen flow generated in electrolytic cells.
- Current control input. This input determines the current that the stack uses to produce hydrogen.
- Electrolytic cell pin - Connect the electrolytic cell stack to the electrical grid. This model assumes an ideal DC/DC converter that converts electrolytic cell voltage to system voltage.
- Electrolytic pin - similar to the electrolytic pin, but instead uses the same principle to connect the compressor. The ideal DC/DC converter between the compressor and the system voltage level.

The model used in this task used the following assumptions.

- The electrolysis process assumes a constant operating point (constant pressure and temperature). The cooling requirements required to maintain the electrolytic cell at a constant temperature are calculated and monitored by the model variable Qdot_cool.
- The compressor operation required for the calculation assumes ideal isothermal compression and constant pressure on the electrolytic cell side (inlet).

LTE model is Semi-Empirical model. The main equation is shown in equations below and is calculated between the current density and the production of electrolysis hydrogen.

Cell Voltage:

$$V_{cell} = V_{rev} + r \cdot J + s \cdot \log_{10}(t \cdot J + 1) \quad (4)$$

Hydrogen flow rate:

$$\dot{n}_{H_2} = \eta_f \cdot n_{cell} \cdot \frac{I}{z \cdot F} \quad (5)$$

The Faraday efficiency:

$$\eta_f = f_2 \cdot \left(\frac{J^2}{f_1 + J^2} \right) \quad (6)$$

Since there is no verification data of LTE model, only the results produced by the model were analyzed.

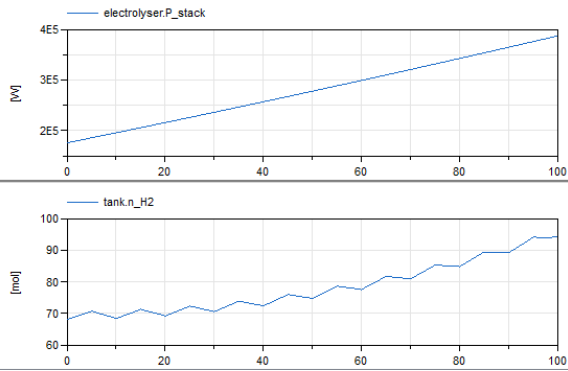


Fig 2.6. Electrolyzer Performance for hydrogen production

2.1.5 Thermal Storage

The thermal storage comprises an indirect thermal energy storage system consisting of a valve, a pump and two tanks with a heat exchanger and the molten salt. Figure 2.7 shows both energy charging and discharging where the heat transfer fluid exchanges energy with the storage system.

The initial temperature of the thermal storage is 240 °C. Heat can be stored up to 290 °C through heat exchange.

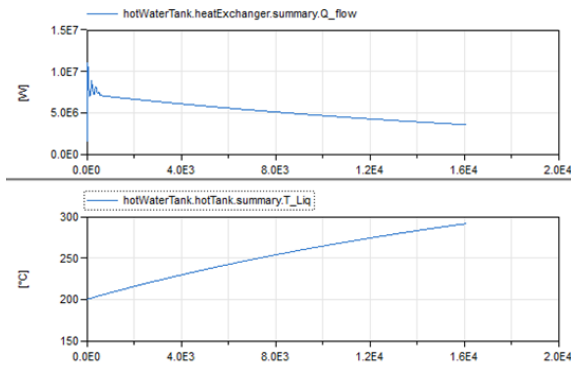


Fig 2.7. Thermal storage sample results

2.1.6. NRHES model Validation

Figure 2.8 is verification system based on Kim [3]. It consists of steam generator, load, battery ESS, etc. Digital twin with identical structure was configured in this task

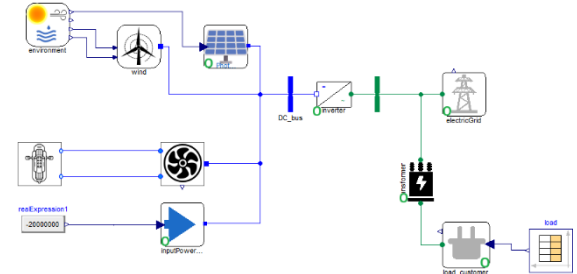


Fig 2.8. NRHES architecture digital twin model

As a result of the model verification, it was confirmed that the reference result and the prediction result provided were within 1% of the error rate in both operation periods. This demonstrates the significance of the digital twin model proposed in this study.

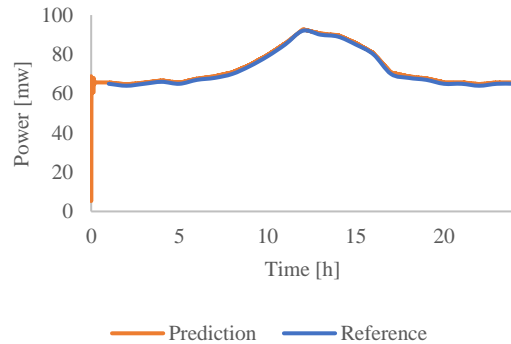


Fig 2.9. Total generation power

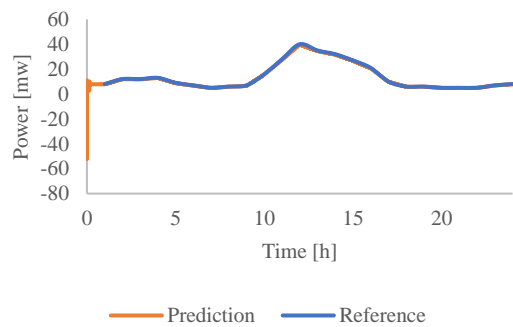


Fig 2.10. Surplus power

2.2. Performance Analysis by NRHES Scenario

Based on battery ESS, thermal storage, and LTE, we analyzed the power production patterns of three NRHES scenarios. Each scenario is expected to help develop an understanding and utilization strategy for

NRHES.

2.2.1. Scenario 01: Add ESS Only

Model

Only battery ESS has been added to the reference model in Chapter 2 with battery ESS Controller. The controller determines the battery charge by monitoring the renewable energy output, surplus power, etc. in real time.

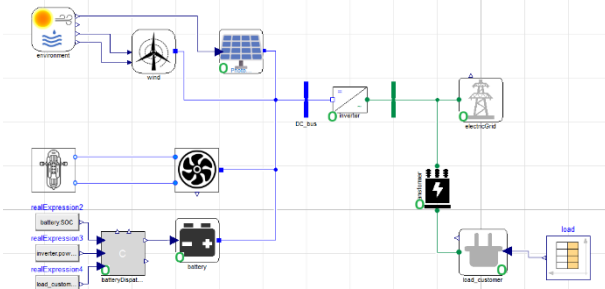


Fig 2.11. Scenario 01 Model

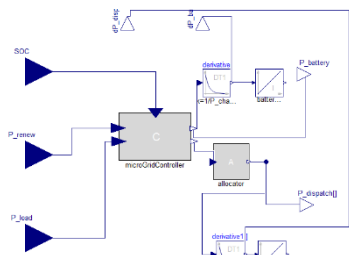


Fig 2.12. ESS Controller Model

Results

Simulation results show a 22% reduction in excess power when using battery ESS. In the absence of energy storage, the excess power is 34.8 MW root-mean-square(rms). When the battery is added, the excess power is 27.3 MWrms.

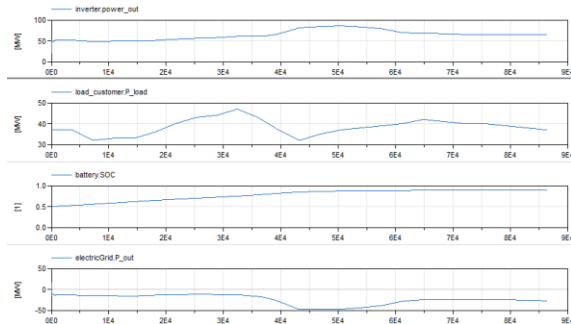


Fig 2.13. Scenario-01 Results

2.2.2 Scenario 02: Scenario 01 + IP added

Model

IP was added to Scenario 01 model. Electrolyzer and controller are also added. The controller determines hydrogen production by monitoring renewable energy production, surplus power, etc. in real time.

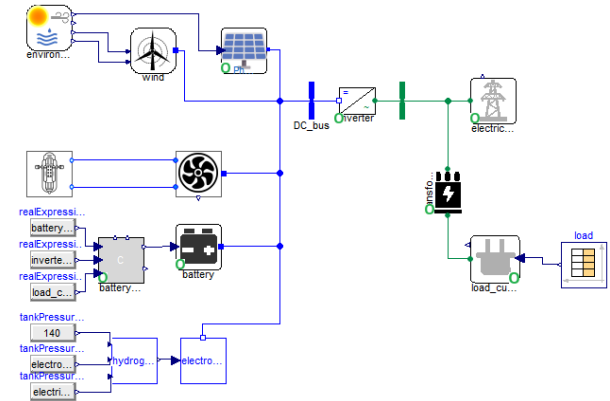


Fig 2.14. Scenario 02 model

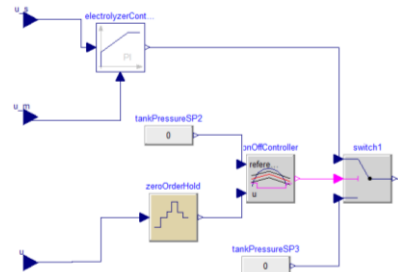


Fig 2.15. Electrolyzer controller

results

Simulation results show a 70% reduction in excess power when using IP. When IP is added, the excess power is 10.64 MWrms.

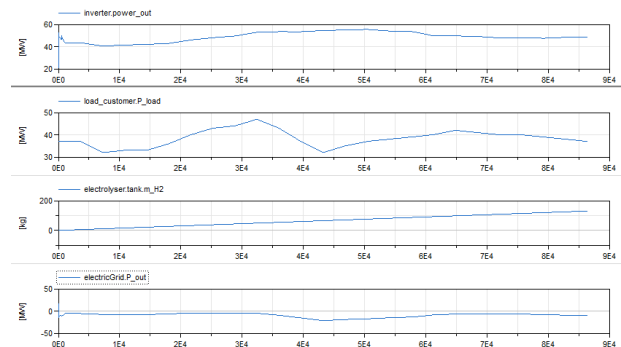


Fig 2.16. Scenario 02 Results

2.2.3 Scenario 03: Scenario 02 + Thermal Storage added

Model

Thermal storage has been added to the Scenario 02 model. In addition, the controller has been modeled. The controller determines the amount of heat exchange by monitoring the renewable energy output, surplus

power, etc. in real time.

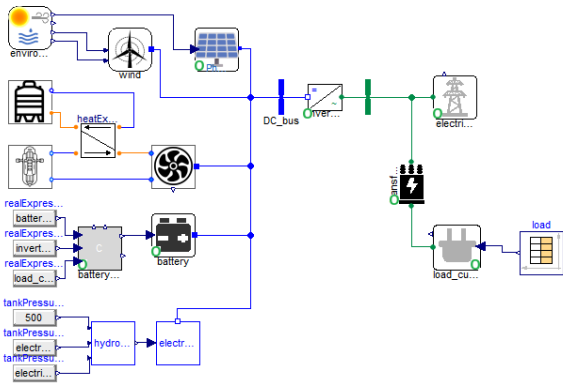


Fig 2.17. Scenario 03 model

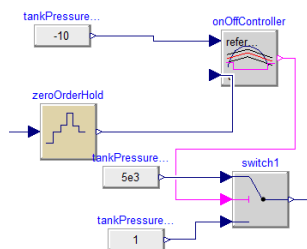


Fig 2.18. Scenario 03 Controller

Results

Simulation results show a 75% reduction in excess power when using IP. When IP is added, the excess power is 9.6 MWrms.

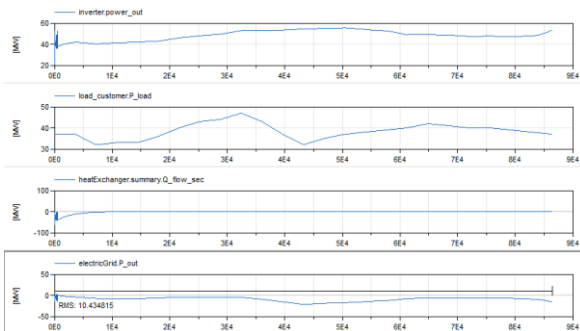


Fig 2.19 Scenario 03 results

3. Conclusions

This paper conducted a study to analyze the performance of NRHES architectures by different scenarios. Digital twin is built based on a multi-physical integrated model using Modelica. The architecture identified three methods according to the strategy for using surplus energy, and the analysis results are as follows.

NRHES was built using the digital twin technology, and research was conducted on the efficiency of each operation strategies.

- Scenario 1: A model that adds battery ESS to the reference model. The battery capacity was set at 20 MWh. As a result of analyzing the efficiency of using surplus power, it was confirmed that 30% was improved compared to the reference model.

- Scenario 2: model that adds low-temperature water electrolysis to the scenario 1 model. The daily hydrogen production was determined to be 130 kg. As a result of analyzing the efficiency of using surplus power, it was confirmed that it was improved by 70% compared to the reference model.

Scenario 3: Model that adds a heat storage device to the Scenario 2. As a result of analyzing the efficiency of using surplus power, it was confirmed that 75% was improved compared to the reference model.

If the cost model is added in the future, it will be possible to study the economics based NRHES architecture and optimal operation scenario.

REFERENCES

- [1] Mark Ruth, Dylan Cutler, Francisco Flores-Espino, and Greg Stark, The Economic Potential of Nuclear-Renewable Hybrid Energy Systems Producing Hydrogen, NREL/TP-6A50-66764, April 2017
- [2] Kim, Jong Suk, Bragg-Sitton, Shannon, Boardman, Richard, Status on the Component Models Developed in the Modelica Framework: High-Temperature Steam Electrolysis Plant & Gas Turbine Power Plant, DO: 10.2172/1333156
- [3] Sung Ho Kim*, Chang Kyu Chung, Hee Hwan Han, Byung Jin Lee, Development of Nuclear-Renewable Hybrid Energy System using Thermal Energy Storage for Industrial Processes, Transactions of the Korean Nuclear Society Autumn Meeting Goyang, Korea, October 24-25, 2019
- [4] Roberto Ponciroli, Yu Tang, and Richard B. Vilim , Characterization of Flexible Operation Performance of N-R HES Components in Support of a Model-Based Pre-conditioner, Philip Eberhart et al., ANL/NE-18/6
- [5] Ruediger Franke and Hansjuerg Wiesmann, Flexible Modeling of Electrical Power Systems – the Modelica PowerSystems Library, Proceedings of the 10th International Modelica Conference, Lund, Sweden, March 10-12, 2014